

Arrested coalescence of multicellular aggregates (Supplementary Figures)

David Oriola,¹ Miquel Marin-Riera,¹ Kerim Anlas,¹ Nicola Gritti,¹ Marina Sanaki-Matsumiya,¹
Germaine Aalderink,¹ Miki Ebisuya,¹ James Sharpe,^{1,2} and Vikas Trivedi^{1,3}

¹*EMBL Barcelona, Dr. Aiguader, 88, 08003, Barcelona, Spain*

²*Institució Catalana de Recerca i Estudis Avançats, 08010, Barcelona, Spain*

³*EMBL Heidelberg, Developmental Biology Unit, 69117 Heidelberg, Germany*

(Dated: March 10, 2022)

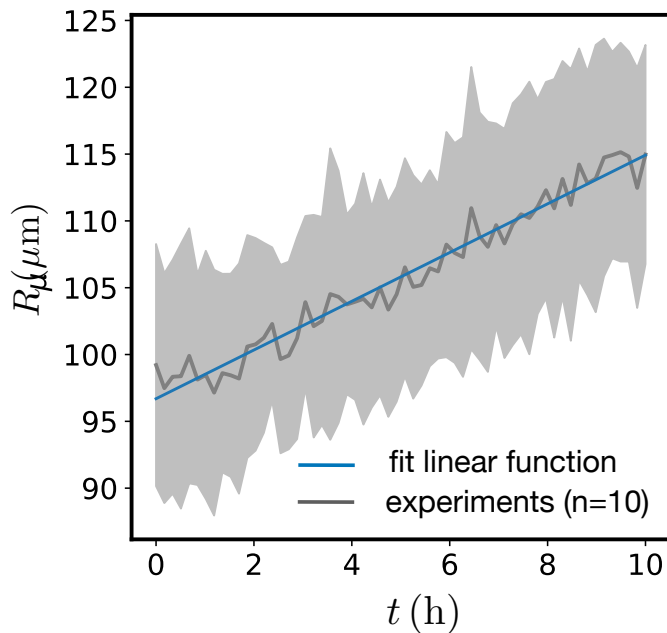


FIG. S1: Average radius of a single mouse aggregate over time ($n = 10$ aggregates, mean \pm SD). The linear fit is used to obtain the doubling time of the cells.

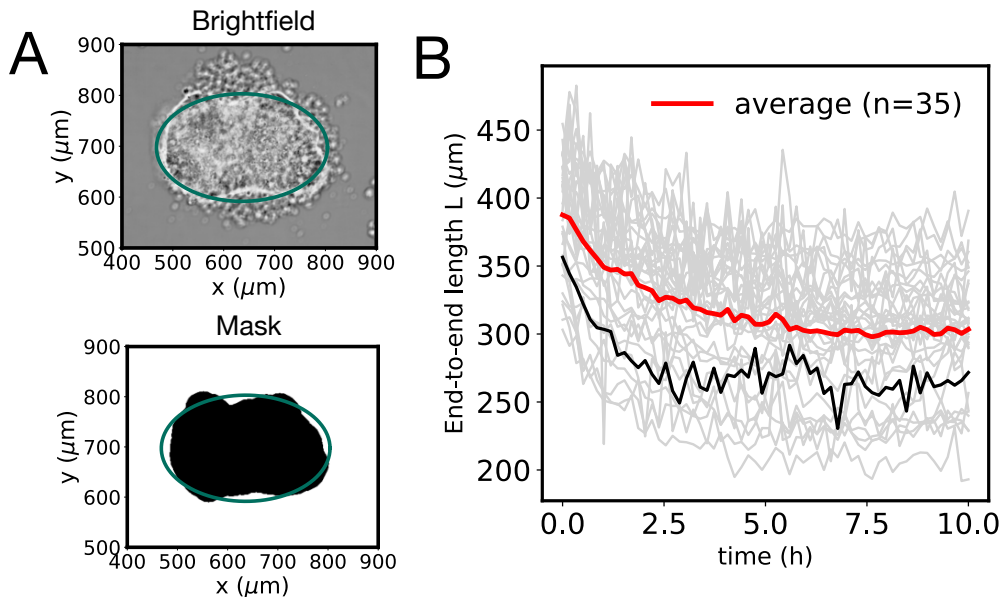


FIG. S2: Image segmentation and determination of the end-to-end length L of the fusion assembly. A) The 2D brightfield images (top) were segmented with the software MORGANA and a final mask was obtained (bottom) for every time point. An ellipse (in green) was fit to the mask at every time point and the end-to-end length L was defined as the major axis of the ellipse. B) Time evolution of the end-to-end length L of 35 fusion events (in light grey) corresponding to the case $R_0 = 96 \pm 10 \mu\text{m}$ in Fig. 3A (Main Text). A representative fusion trajectory is highlighted in black and the averaged curve is shown in red.

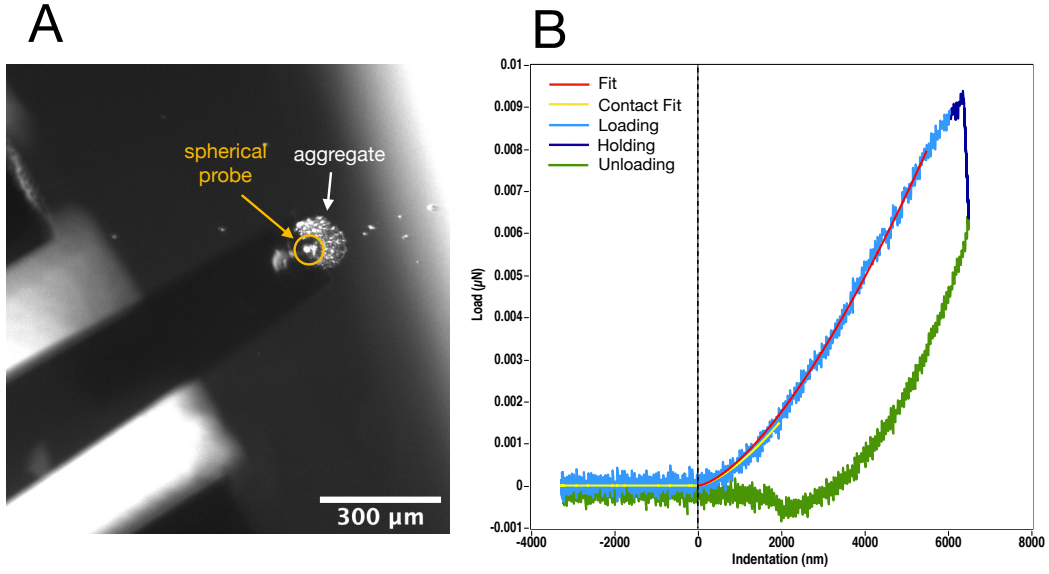


FIG. S3: Nanoindentation. A) Bright field image of a 24h mouse embryonic stem cell aggregate in NDiff227 medium under the Chiaro Nanoindenter. B) Typical indentation curve with a maximal force of $\sim 0.01 \mu\text{N}$ and maximum indentation depth of $\sim 7 \mu\text{m}$. The fits correspond to the Herz's model considering a spherical tip.

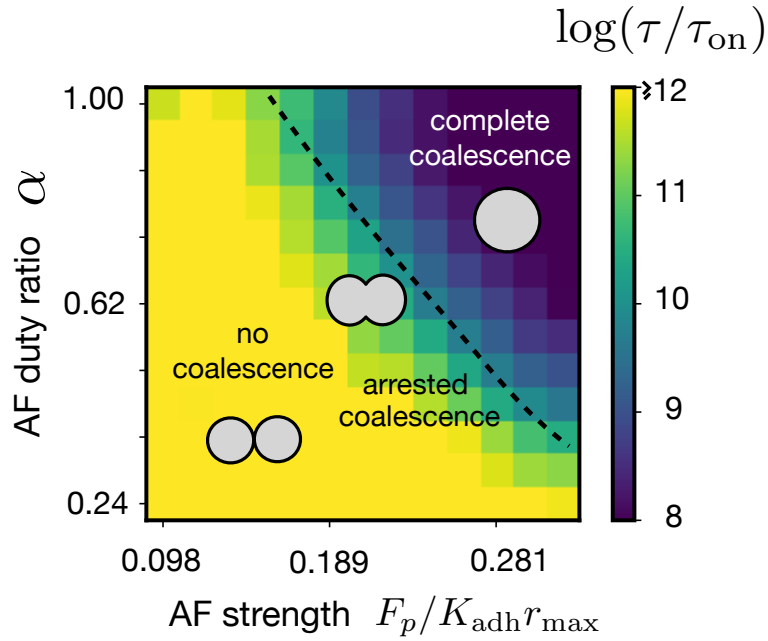


FIG. S4: Colormap of the logarithm of the dimensionless viscopillary time $\log(\tau/\tau_{\text{on}})$ as a function of the the duty ratio α and strength $F_p/(K_{\text{adh}} r_{\text{max}})$ of active fluctuations (AF). The parameters are the same as in Fig. 4 in the Main Text.

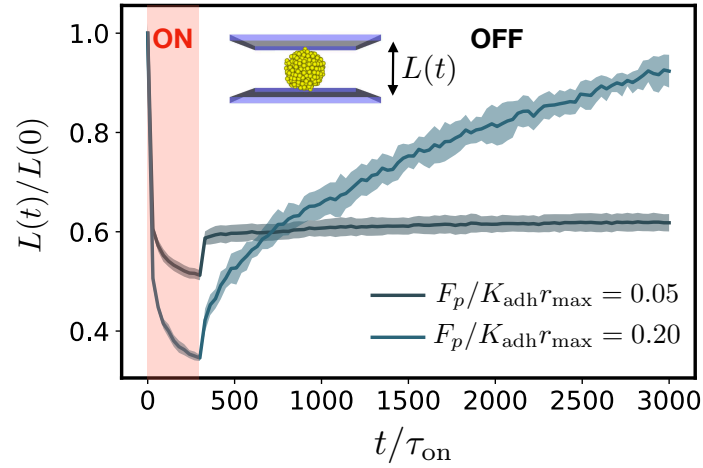


FIG. S5: Parallel plate compression simulations using the software ya||a. The axial deformation of the aggregate $L(t)/L(0)$ (mean \pm SD, $n = 9$) is studied considering jammed ($F_p/(K_{\text{adh}}r_{\text{max}}) = 0.05$) and unjammed ($F_p/(K_{\text{adh}}r_{\text{max}}) = 0.20$) cell aggregates of 500 cells each. $K_{\text{adh}}/K_r = 1$, $\alpha = 1$, $\lambda/K_{\text{adh}}\tau_{\text{on}} = 1$. In the red region, a compressive force $F/(K_{\text{adh}}r_{\text{max}}) = 10$ is applied. See corresponding Movies S5 and S6.

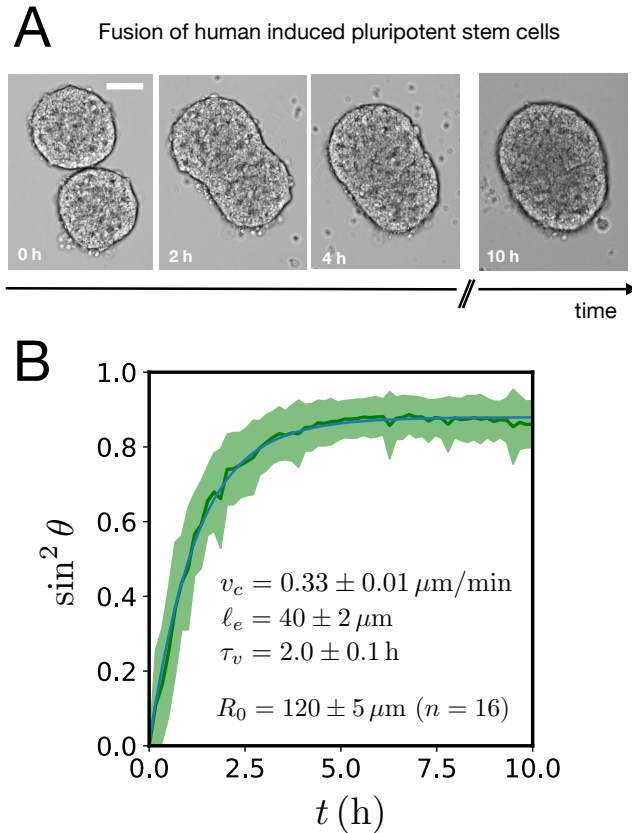


FIG. S6: Fusion of human induced pluripotent stem cell (hiPSCs) aggregates at 24h after aggregation. The number of cells per aggregate was ~ 500 during aggregation. A) Sequence of snapshots showing a fusion event of hiPSCs. Scale: $100 \mu\text{m}$. B) Average curve of $\sin^2 \theta$ vs time for $n = 16$ fusion events with an average radius of $R_0 = 120 \pm 5 \mu\text{m}$ (mean \pm SD). The estimated values of v_c , ℓ_e and τ_v are shown.

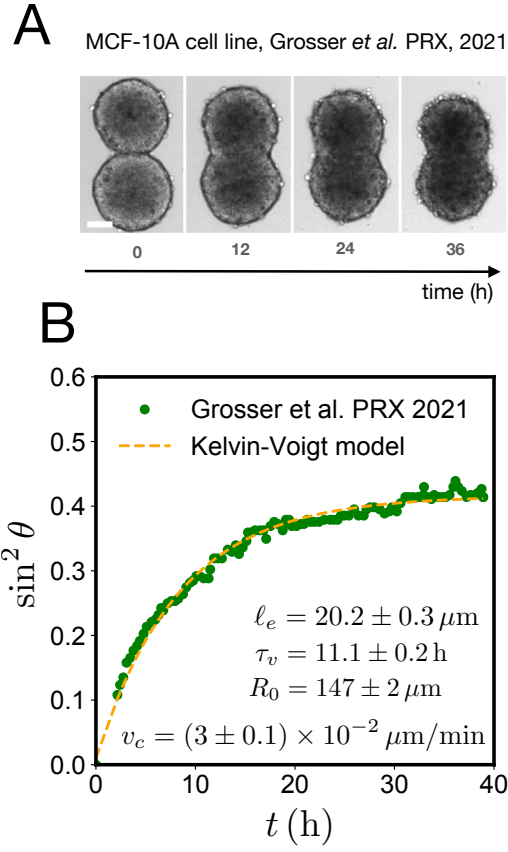
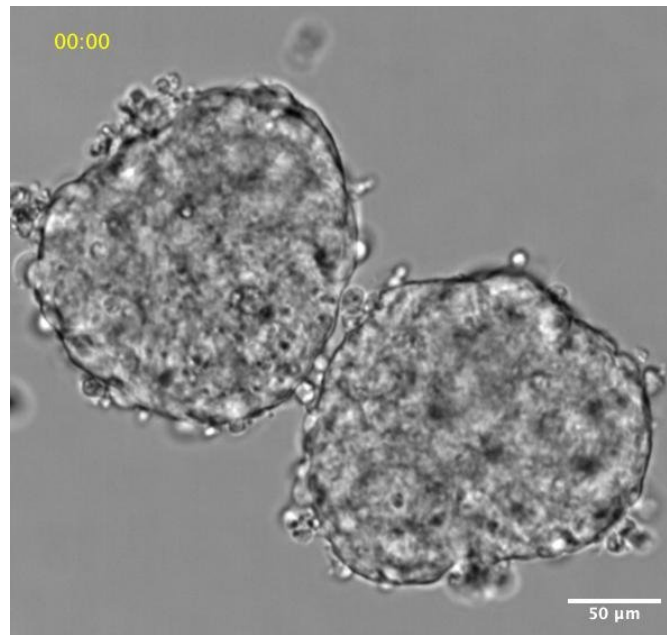
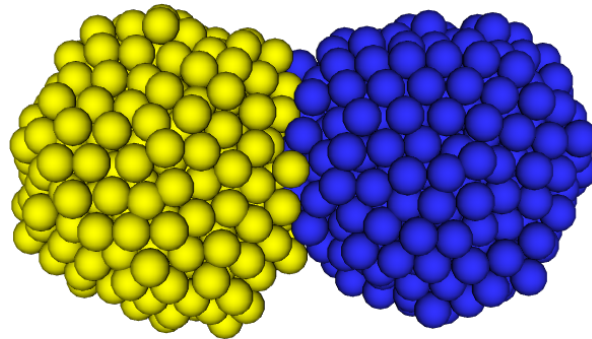


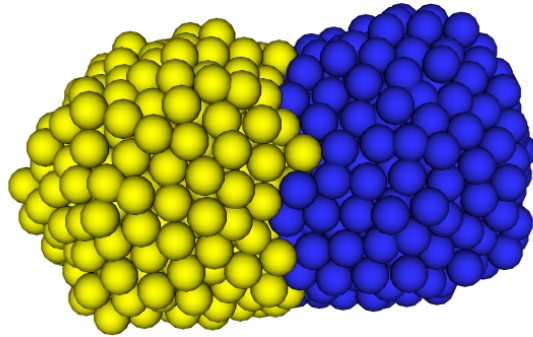
FIG. S7: Fusion of human epithelial breast cell (MCF-10A) aggregates in Grosser *et al.* PRX, 2021. A) Series of snapshots during the fusion process (adapted from Grosser *et al.* PRX, 2021). Scale bar: $100 \mu\text{m}$. B) Analysis of the MCF-10A fusion data from Fig. 2C in Grosser *et al.* PRX, 2021 and fit to a Kelvin-Voigt model. We observe that our model successfully captures the observed arrested coalescence dynamics. The data was digitized using WebPlotDigitizer. Given that fusion already started in the first time point in Fig. 2C from Grosser *et al.* PRX, 2021, we introduced a 2h time gap for the fit.



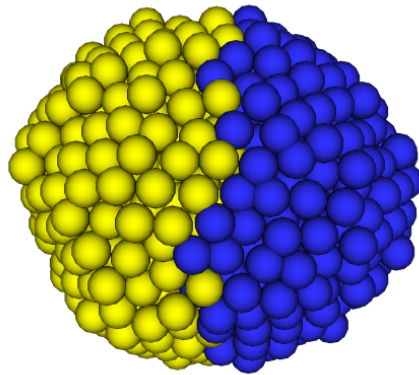
Movie S1. Brightfield timelapse of the fusion of two mouse embryonic stem cell aggregates 24h after aggregation. 10x air objective and 0.3 N.A. The movie corresponds to the snapshots shown in Fig. 1C.



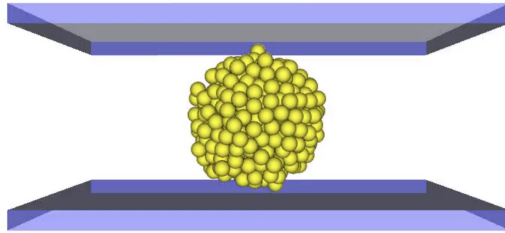
Movie S2. ya||a simulation showing no coalescence. 500 cells per aggregate, $K_{\text{adh}}/K_r = 1$, $\alpha = 1$, $F_p/(K_{\text{adh}}r_{\text{max}}) = 0.10$ and $\lambda/K_{\text{adh}}\tau_{\text{on}} = 1$. Total time $4000\tau_{\text{on}}$.



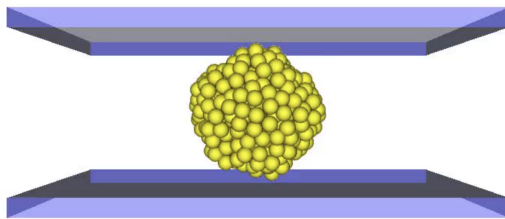
Movie S3. ya||a simulation showing arrested coalescence. 500 cells per aggregate, $K_{\text{adh}}/K_r = 1$, $\alpha = 1$, $F_p/(K_{\text{adh}}r_{\text{max}}) = 0.15$ and $\lambda/K_{\text{adh}}\tau_{\text{on}} = 1$. Total time $4000\tau_{\text{on}}$.



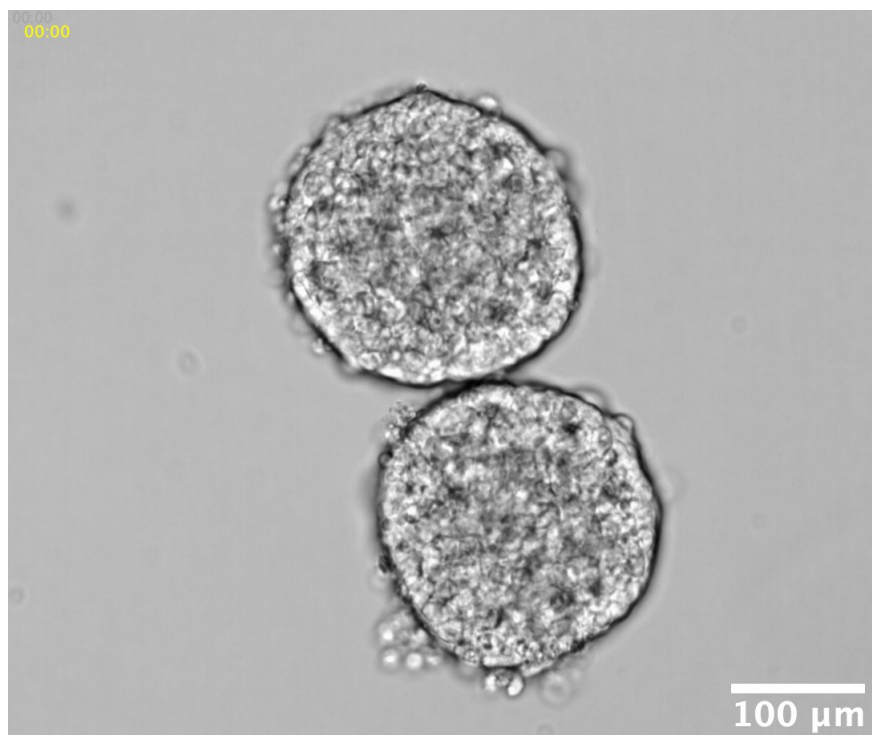
Movie S4. ya||a showing complete coalescence. 500 cells per aggregate, $K_{\text{adh}}/K_r = 1$, $\alpha = 1$, $F_p/(K_{\text{adh}}r_{\text{max}}) = 0.20$ and $\lambda/K_{\text{adh}}\tau_{\text{on}} = 1$. Total time $4000\tau_{\text{on}}$.



Movie S5. ya||a simulation showing no recovery of a 500 cells aggregate in the jammed (solid) regime. $K_{\text{adh}}/K_{\text{r}} = 1$, $\alpha = 1$, $F_p/(K_{\text{adh}}r_{\text{max}}) = 0.05$, $F/(K_{\text{adh}}r_{\text{max}}) = 10$ and $\lambda/K_{\text{adh}}\tau_{\text{on}} = 1$.



Movie S6. ya||a simulation showing complete recovery of a 500 cells aggregate in the unjammed (fluid) regime. $K_{\text{adh}}/K_{\text{r}} = 1$, $\alpha = 1$, $F_p/(K_{\text{adh}}r_{\text{max}}) = 0.20$, $F/(K_{\text{adh}}r_{\text{max}}) = 10$ and $\lambda/K_{\text{adh}}\tau_{\text{on}} = 1$.



Movie S7. Brightfield timelapse of the fusion of two hiPSC aggregates at 24h. 10x air objective and 0.3 N.A.